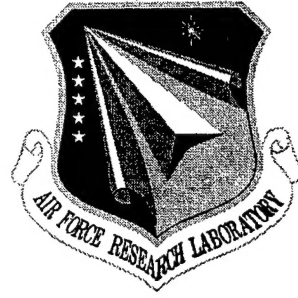AFRL-SN-RS-TR-1998-227
Final Technical Report
January 1999

TUNABLE WAVELENGTH-BASED PHOTONIC ARCHITECTURES FOR THE DYNAMIC CONTROL OF PHASED ARRAY ANTENNAS

University of Florida
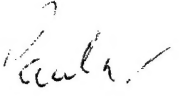
Henry Zmuda

19990209 063

APPROVED FOR PUBLIC RELEASE; DISTRIBUTION UNLIMITED.

**AIR FORCE RESEARCH LABORATORY
SENSORS DIRECTORATE
ROME RESEARCH SITE
ROME, NEW YORK**

This report has been reviewed by the Air Force Research Laboratory, Information Directorate, Public Affairs Office (IFOIPA) and is releasable to the National Technical Information Service (NTIS). At NTIS it will be releasable to the general public, including foreign nations.

AFRL-SN-RS-TR-1998-227 has been reviewed and is approved for publication.

APPROVED:

PAUL M. PAYSON
Project Engineer

FOR THE DIRECTOR:

ROBERT G. POLCE, Acting Chief
Rome Operations Office
Sensors Directorate

REPORT DOCUMENTATION PAGE

1. AGENCY USE ONLY (Leave blank)	2. REPORT DATE	3. REPORT TYPE AND DATES COVERED
	January 1999	Final Jan 96 - Mar 98

4. TITLE AND SUBTITLE
TUNABLE WAVELENGTH-BASED PHOTONIC ARCHITECTURES FOR THE DYNAMIC CONTROL OF PHASED ARRAY ANTENNAS

6. AUTHOR(S)

Henry Zmuda

5. FUNDING NUMBERS
C   -   F30602-96-2-0046
PE -   62702F
PR -   4600
TA -   P5
WU -   PA

7. PERFORMING ORGANIZATION NAME(S) AND ADDRESS(ES)
University of Florida
Division of Sponsored Research
219 Grinter Hall
Gainesville FL 32611

8. PERFORMING ORGANIZATION REPORT NUMBER

N/A

9. SPONSORING/MONITORING AGENCY NAME(S) AND ADDRESS(ES)

Air Force Research Laboratory/SNDR
25 Electronic Parkway
Rome NY 13441-4515

10. SPONSORING/MONITORING AGENCY REPORT NUMBER

AFRL-SN-RS-TR-1998-227

11. SUPPLEMENTARY NOTES

Air Force Research Laboratory Project Engineer: Paul M. Payson/SNDR/(315) 330-7911

12a. DISTRIBUTION AVAILABILITY STATEMENT

Approved for public release; distribution unlimited.

12b. DISTRIBUTION CODE

13. ABSTRACT (Maximum 200 words)
This report examines three novel photonic systems for controlling broadband phased array antennas. These photonic systems take advantage of recent advances in fiber Bragg gratings, high dispersion optical fiber and tunable wavelength laser technologies. The first system is a transmit/receive beamformer that uses fiber gratings arranged in a prism-like configuration. A proof-of-concept breadboard for controlling a three-element phased array antenna demonstrated high-resolution beamsteering over a 3.5 GHz bandwidth. Based on this discrete architecture, two other systems are proposed; a transversal filter and an optical packet encoder/decoder for optical data communication systems. The second system utilizes high dispersion optical fiber along with fiber Bragg gratings to achieve continuous steering for both transmit or receive. The system, dubbed a photonic crossbar switch, allows the independent routing of a wavelength-encoded signal from an arbitrary input port to an arbitrary output port. The third system, a modified version of the crossbar switch, is capable of broadband null steering. Measurements taken over a ten-percent fractional bandwidth on a three-element proof-of-concept system showed a uniform null depth of better than 40 dB across the entire band. The architecture presented is best suited for small antenna array applications, for example GPS-guided airborne munitions.

14. SUBJECT TERMS
Phased Array Antennas, True Time Delay Beamforming, Broadband Microwave Signals, Broadband Null Steering, Transversal Filter, Optical Packet Encoder, Photonics, Fiber Bragg Reflective Gratings, High Dispersion Optical Fiber

15. NUMBER OF PAGES
40

16. PRICE CODE

17. SECURITY CLASSIFICATION OF REPORT	18. SECURITY CLASSIFICATION OF THIS PAGE	19. SECURITY CLASSIFICATION OF ABSTRACT	20. LIMITATION OF ABSTRACT
UNCLASSIFIED	UNCLASSIFIED	UNCLASSIFIED	UL

ABSTRACT

This report examines three novel systems that utilize photonic processing techniques for broadband microwave signals applied to the control of a phased array antenna. The photonic systems take advantage of recent advances in fiber Bragg gratings, high dispersion optical fiber, and tunable wavelength laser technologies. Both fiber Bragg gratings and high-dispersion optical fiber have emerged as efficient, versatile, cost effective photonic components. Systems employing these components they hold the promise of revolutionizing the field of broadband photonic processing and practical commercial photonic processors are likely to become viable in the near term.

Specifically, this report examines three systems in detail. The first is a transmit/receive beamformer that uses fiber Bragg gratings arranged in a prism-like configuration. The system is capable of steering an electromagnetic beam at fixed (discrete) spatial angles. A proof-of-concept system for controlling a three-element phased array antenna was constructed. Measurements taken over a 3.5GHz bandwidth demonstrates high-resolution beamsteering and highly linear low-noise phase data. Based on the discrete architecture, two other systems are proposed; a transversal filter and an optical packet encoder/decoder for optical data communication systems.

The second system considered can be regarded as the continuous version of the previous discrete beamformer. This system utilized high dispersion optical fiber along with fiber Bragg ratings to achieve continuous steering of an electromagnetic beam in space. The system is dubbed a photonic crossbar switch since it allows the independent routing of a wavelength-encoded signal from an arbitrary input port to an arbitrarily selected output port. This report demonstrates how this system can be used as a efficient transmit/receive beamforming architecture.

The third system studied in this report is really a modified version of the second system, the crossbar switch, and shows how this modified system can be used in the important application of broadband null steering. For the null steering application, measurements taken over a ten-percent fractional bandwidth on a three-element proof-of-concept system shows a null depth of better than 40 dB uniform across the entire band in this laboratory setup. The architecture presented is best suited for small antenna array applications, for example self- or GPS-guided airborne munitions. In a fully integrated, optimized system, null depths of 50 dB or greater across a multi-gigahertz bandwidth are anticipated and the critical factors which influence this performance are examined.

All architectures presented take maximum advantage of component reuse and fully integrate the receive, and where appropriate, transmit mode of operation in one efficient hardware compressive topology.

TABLE OF CONTENT

TABLE OF FIGURES

1 INTRODUCTION

The use of dynamic techniques to electronically steer the aperture of a phased array antenna system has long been a topic of great interest. A phased array has the ability to focus beams in specified spatial coordinates while simultaneously placing nulls along other spatial coordinates making it immune to jammers, intentional or otherwise, and providing a significant reduction in multi-path interference, a problem of great concern in most communications applications [1,2].

Electronic processing systems used to accomplish this beamsteering have not been without their problems, however. Microwave circuit components tend to be cumbersome, especially at lower microwave frequencies. This has limited the widespread use of large phased arrays especially in airborne applications where size and weight are primary concerns. Another significant limitation is that the microwave circuit components needed to implement a beamformer are inherently narrowband, limiting the bandwidth of the beamforming system to a few percent of the RF carrier frequency. The use of narrowband components results in a beampointing error known as *squint*, where each frequency component points in a different spatial direction. Modern radar tracking and surveillance systems and Electronic Support Measures (ESM) require wideband performance (2-18 GHz bandwidth is a commonly stated requirement) making phase-steered systems less than ideal.

The only way to make a phased array "broadband" is to employ true-time delay beamforming techniques. An array aperture is "steered" by applying an appropriate amount of time delay to each signal used to drive the elements of the array. The only way to achieve time-delay of a microwave signal, short of digitizing it and storing it in a computer memory[1] for later re-construction is to provide an appropriate path length for the signal to propagate. Reconfigurable beamsteering requires a variable length line, the practical implementation of which has been a challenging problem.

In recent years, optical processing techniques for microwave signals have made significant advances in the area of phased array antenna control. Several advantages of optical processing techniques are often touted, such as reduced weight and increased immunity to EMP and EMI effects. Yet beyond these advantages, perhaps the greatest contribution of optical processing techniques for phased arrays will be its ability to incorporate true-time delay beamforming methods in some rather innovative ways. Recent developments in both in-fiber optical components and optical integrated circuits has led to optically controlled phased array architectures which could provide a field-worthy system in the short term. Recent advances in permanent fiber-based Bragg reflection gratings (BRG's) have allowed these devices to become an off-the-shelf product [9]. BRG's show great promise for microwave delay line technology and have been proposed for use in phased array transmit/receive systems. With developments in tunable wavelength laser technology, systems utilizing highly dispersive optical fiber to achieve

---

[1] Digital Signal Processing (DSP) techniques are limited by the bandwidth of analog-to-digital converters, which typically have a bandwidth of several hundred megahertz. Wideband microwave signals thus require the use of sub-band coding techniques resulting in a computationally intensive processing problem for broadband phased array systems.

a variable microwave delay line were studied [4]. These systems are fiber-based and therefore have the distinct advantage of being able to incorporate fiber amplifiers directly in the system, thereby allaying some of the concerns that occur when a single laser source is distributed to the (potentially) many channels of a phased array system.

This report presents several innovative architectures for phased array antennas that utilize BRG's and High Dispersion Optical Fiber (HDOF) as a fundamental processing element [28]. It is also shown how similar BRG/HDOF based systems can be used to accomplish other types of RF signal processing tasks. Both continuous and discretely variable true-time-delay beamformers are presented, with the former being especially useful for null steering applications. The architectures described in this paper are simple enough to make them an attractive approach even for narrowband applications where a only simple RF/microwave phase shifter is necessary.

Though much attention has been given to the use of optically generated true time delay for broadband phased array beamforming as described above, much less attention however has been given to the important ability of a phased array to place broadband nulls at chosen angular coordinates. This is because most optical processors generally do not possess the necessary flexibility needed to independently steer arbitrary nulls. One requirement needed for null steering is the ability to vary the time delay in a continuous rather than discrete fashion, and thus a particularly attractive approach is the dispersive fiber prism proposed by Frankel and Esman [3]. The approach utilizes a continuously tunable laser to access the variable time delay obtainable from a high chromatic dispersion optical fiber. Soref utilized a similar approach to obtain a generic variable delay line for broadband applications.

This report shows a novel tunable laser-based true time delay processor for a phased array receiver with broadband adaptive nulling capability. The nulling architecture described here has several distinct advantages. The system is entirely fiber-based, and only a single length of high dispersion optical fiber is needed for the entire system. This single fiber approach makes the performance especially insensitive to temperature drift (normally a problem of great concern in such systems) and greatly helps to maintain the extremely accurate element-to-element amplitude and phase tracking needed for deep nulls [5]. For example, to obtain a 60-dB null depth, element-to-element gain and phase variation must be kept to better than 0.01 dB and 0.025-degrees, respectively. Equalization between the optical channels is more easily maintained, compared to conventional IF or baseband processors, by operating on the raw broadband optical signal components. Narrow band filters, such as SAW filters or ceramic filters, that significantly degrade channel equalization in conventional nullsteering processors are not used until after the antenna channels are optically combined. Finally, the wide varieties of classical adaptation algorithms normally associated with narrowband applications are equally applicable to this broadband implementation. For example, a digital gradient-search adaptation algorithm can control the optically implemented delays using the digitized antenna outputs as feedback. The algorithm would simultaneously iterate through multiple steering vectors to rapidly converge to a solution [7].

2

2 COMPONENT OVERVIEW

2.1 High Speed Tunable Laser Technology

A critical component of a wavelength-controlled optical processor is the wavelength tunable optical source. Recent interest in the application of photonic processing methods for wavelength division multiplexing (WDM) telecommunications systems has led to a proliferation in research in tunable laser technology. Trends in WDM communication indicate that a broadly tunable laser capable of random wavelength access will play a key role in future systems [15].

In addition to the usual concerns for laser selection in photonic systems, the applications studied here pose additional requirements with regard to wavelength range and tuning speed. Semiconductor lasers often consist of an active gain medium that is spectrally broad and that defines the free spectral range (FSR) over which the laser may be frequency tuned. A cavity structure containing a wavelength selective element establishes the operating wavelength of the laser. Several methods exist for modifying the operating wavelength via modulation of the wavelength selective element [16]. One approach is by (rapidly) varying the index of an etalon contained within the cavity. This type of electro-optic tuning is range limited to less than 2 THz (16 nm at a 1.55 µm center wavelength) since only small index changes are possible. Mechanical tuning is another approach which can achieve extremely broad tuning ranges but is generally very slow (KHz ~ low MHz range). Large, rapid wavelength variation may be obtained by modulating the angle at which the light travels in the cavity thereby changing the physical path length. This angle modulation can be performed with a variety of beam deflection techniques ranging from electro-optic beam deflectors to acousto-optic deflectors or surface acoustic wave (SAW) devices. One fiber laser-based approach uses acoustooptic tunable filters to achieve rapid, broad range tuning. These systems tend to be bulky and require large control power levels [18,19].

Other approaches include externally addressable Fabry-Perot devices and birefringent tuning via Pockel cells. Mach-Zehnder based Y-branch lasers are capable of rapid wideband tuning with a single control current [17]. Distributed Bragg Reflector (DBR) lasers are passively tuned and have a continuous or discrete tuning range of about ten nanometers, limited by carrier lifetimes. Distributed Feedback (DFB) lasers have an active tuning region that results in much shorter carrier lifetimes. Tuning speeds of less than one nanosecond are possible but at the expense of a smaller tuning range. Both the DBR and DFB lasers rely on the fractional index change from the electro-optic effect to tune [20,21].

Attempts to obtain broad tunability at high speed are being pursued by several researchers. Laser structures such as Vertical Grating Assisted Coupler lasers can currently achieve a tuning range of 50 nm with larger ranges expected. Super Structure Grating DBR lasers can currently achieve 100 nm tunability. Both these technologies can currently tune at rates of less than 10 nanoseconds. Another way to overcome the conflict between switching time and tunability is to switch among laser diodes with a high-speed switching matrix. One such approach used for WDM applications utilizes electroabsorption optical switching to achieve a wavelength switching time of about 10 picoseconds [22].

The need for small, efficient, inexpensive, high-speed broadly tunable lasers is being driven primarily by the WDM community and improvements realized there will directly benefit microwave-photonic signal processing systems as well

2.2 Bragg Reflection Gratings (BRG)

An integral component of the processor portion of the photonic systems presented in this paper is the BRG. Recent advances in BRG technology coupled with efficient manufacturing methods have allowed the BRG to become a commercial off-the-shelf product. Exposing a hydrogen-loaded silica fiber to a periodic pattern produced with either a mask or an interference pattern using an intense ultraviolet laser generally makes reflection gratings. This exposure causes a periodic phase grating to be permanently written into the core and cladding of the fiber. For wavelengths within the transmission stop band, the grating couples energy from the incident wave into the corresponding reflected wave. The magnitude of the UV induced index deviation and the length of the grating, which are readily controlled design parameters, determine the BRG's spectral bandwidth and reflectivity. Devices with reflection bandwidths as narrow as 0.02 nanometers or as broad as 100 nanometers are available from several manufacturers. Using a chirped rather than periodic index variation obtains broad reflection bandwidths. Reflectivity at the Bragg wavelength can be designed to be as low as 1% or greater than 99.9%. Off-wavelength transmission is nearly 100%. Consequently, BRG's are an extremely efficient and versatile optical design element [10,11,12].

2.3 High Dispersion Optical Fiber

As light propagates along a single mode optical fiber, it experiences a group delay τ_g (with corresponding group velocity v_g)

$$\tau_g = \frac{1}{v_g} = \frac{dk}{d\omega} \tag{1}$$

where $k = \frac{n(\omega)\omega}{c}$ is the wavenumber, $n(\omega)$ is the refractive index of the fiber which in general is a function of frequency, c is the speed of light in free space, and $\omega = \frac{2\pi f}{c} = \frac{2\pi}{\lambda}$ where ω is the radian frequency with λ the free space wavelength.

Substituting into Equation (1) and differentiating we obtain

$$\tau_g = \frac{N_g}{c} \tag{2}$$

where the quantity

$$N_g = n + \omega \frac{dn}{d\omega} = n - \lambda \frac{dn}{d\lambda} \tag{3}$$

4

is known as the *group index*. Note that for an ideal frequency independent index n_o (dispersionless) fiber, the group delay is simply

$$\tau_g = \frac{n_o}{c} \qquad (4)$$

Consider then two wavelengths λ_1 and λ_2 propagating on the same fiber. After travelling a distance L they will each wavelength experiences a different time delay, $\tau_1 = L\dfrac{N_g(\lambda_1)}{c}$ and $\tau_2 = L\dfrac{N_g(\lambda_2)}{c}$ and thus experience a *differential* time delay $\Delta\tau$ equal to

$$\Delta\tau = \frac{L}{c}(N_g(\lambda_1) - N_g(\lambda_2)) = \frac{L}{c}\frac{dN_g(\lambda)}{d\lambda}\Delta\lambda \qquad (5)$$

where $\Delta\lambda = |\lambda_1 - \lambda_2|$ and $\dfrac{dN_g(\lambda)}{d\lambda} = -\lambda\dfrac{d^2n(\lambda)}{d\lambda^2}$

The differential time delay can thus be written

$$\Delta\tau = -\frac{L}{c}\lambda\frac{d^2n(\lambda)}{d\lambda^2}\Delta\lambda \qquad (6)$$

The quantity $D = -\dfrac{\lambda}{c}\dfrac{d^2n(\lambda)}{d\lambda^2}$ is known as the *dispersion* and it is the quantity which is exploited in high dispersion optical fiber [8]. Special optical fiber manufacturing techniques allow dispersion values of greater than −100 picoseconds/nanometer-kilometer while standard fiber has a dispersion of less than +20 psec/nm-Km. This means that substantial differential time delays can be obtained by utilizing the wavelength-dependent time delay obtained from the high dispersion optical fiber.

3   PHASED ARRAY BEAMFORMING

3.1   True-Time-Delay Beamforming Systems

The general theory for broadband beamforming is well documented in the open literature [14]. It is well known that for an N-element true-time-delay (TTD) phased array beamformer the signal to be transmitted is split N times, time delayed by appropriate amounts, and distributed to the antenna radiating elements. For example, the array factor for a linear array of N equally spaced isotropic radiators which produces a far-field pattern which propagates at an angle $\theta = \theta_o$ off broadside is well known and given by

$$F(\theta) = \sum_{n=1}^{N} a_n \exp[jnsk_o(\sin \theta - \sin \theta_o)] \tag{7}$$

where a_n is a constant phasor amplitude, s is the antenna element spacing, $k_o = 2\pi f_m/c_o$, f_m is the microwave frequency, c_o is the speed of light in free space, and $-\pi \leq \theta \leq \pi$. It is seen that phase shift required to steer each frequency component at the angle θ_o is a linear function of frequency requiring a time delay Δt_n of

$$\Delta t_n = n\frac{s}{c}\sin \theta_o \tag{8}$$

Antenna reciprocity can be invoked to demonstrate similar results for the receive mode of operation. A dynamically steered array requires the ability to vary the time delay. More demanding applications such as adaptive nulling systems yield optimal performance only when the differential time delay Δt_n can be varied in a continuous rather than discrete fashion.
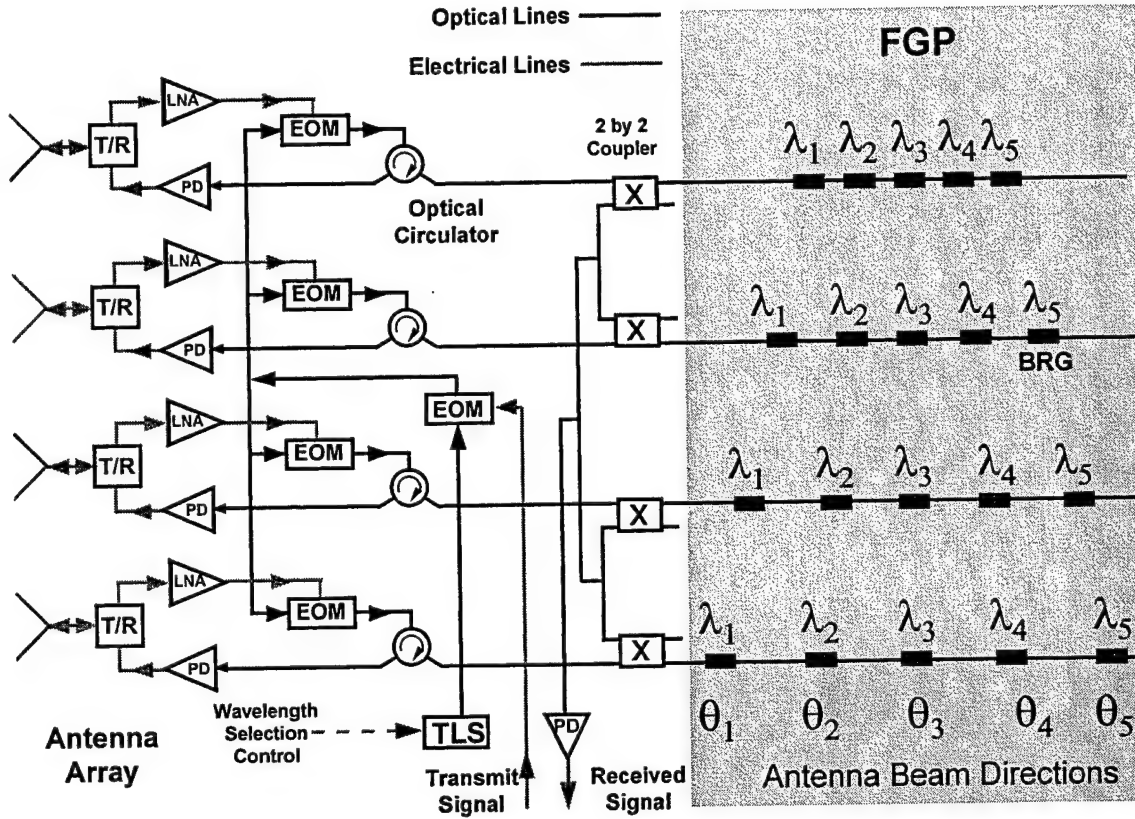
4 DISCRETE BEAMFORMING SYSTEM

4.1 Fiber Grating Prism Beamformer

The system level diagram for a N *by* M two-dimensional beamformer is shown in Figure 1. For the transmit mode of operation the outputs of a set of M tunable laser sources (TLS) are externally modulated using M electrooptic modulators (EOM). This modulated light feeds a group of N single-mode fibers through a set of M equal-path 1:N power dividers. The receive EOM's are not used in the transmit mode. Optical circulators are used to direct the modulated signals to the fiber grating prism (FGP). Each fiber includes a spatially distributed array of BRG's which collectively form the FGP. The different peak-reflection wavelengths $\lambda_1 \ldots \lambda_L$ of the various gratings are within the tuning range of the laser $\Delta\lambda$. Reflected light is time-delayed in accordance with the particular grating addressed. The light is then routed by the optical circulators to the antenna backplane where the signals are detected, amplified, and sent to the antenna elements.

In the receive mode the TLS feeds N *by* M optical channels with unmodulated light. The received microwave signals are directed to a set of N *by* M EOM's. The modulated optical signals are then directed to the FGP via the optical circulators. These properly delayed optical signals are summed together and sent to a PD for recovery of the collective microwave signal. Wavelength selection in the TLS selects a desired outgoing as well as incoming beam direction. In essence, the FGP receive system acts as a matched filter.

To understand the basic design details of the FGP circuit assume a simplified one-dimensional array (M = 1) of uniformly spaced radiators a distance s apart. The main lobe of the phased-array antenna will be designed to point in any one of L discrete as selected by the laser wavelength. A far-field plane wave will propagate from the array in a direction θ_i (measured with respect to broadside) when a differential time delay $\Delta t_i = (s/c_o) \sin \theta_i$ is established between adjacent radiators. The FGP provides the desired group of differential delays Δt_{ij} by a set of

double pass delays to-and-from the next grating: $\Delta t_{ij} = 2d_{ij}n/c_o$, where d_{ij} is the spacing between the center of the i-th grating in fiber j and the center of the broadside grating in fiber j, n (≈ 1.5) is the fiber waveguide index, i = 1, 2, 3, ..., L and j = 1, 2, 3, ..., N.

FIGURE 1: FIBER GRATING PRISM DISCRETE TRANSMIT/RECEIVE BEAMFORMING ARCHITECTURE.

Regarding system loss, the laser power reaching the PD's in Figure 1 is reduced by several factors in both the transmit and receive mode of operation. The FGP introduces a loss 1 - R, where R is the reflectance of the selected grating. The reflectance of the BRG's can be greater than 99%, while the M - 1 (maximum) unselected gratings per channel do not introduce appreciable optical loss. The major loss mechanisms are the 1:N splitter/summer (10 log N dB), the circulator (1 dB per direction), and the couplers (6 dB round trip). Note that the receive mode experiences additional loss due to a second summer. Generally, an EOM biased at quadrature contributes a total insertion loss of approximately 6 to 8 dB. Note also that in the receive mode, the transmit EOM, though present, is not used, and vice versa. Splices, connectors, isolators, polarization control, and the like will add another few dB of excess loss to the system. Detector responsivity will contribute minimally to signal loss, and in some cases provide gain. The total loss is the sum of the above, and the RF loss is twice the optical loss. Since the system is fiber-based, optical amplifiers can be incorporated into the design to compensate for the losses in the system. It is also necessary to maintain uniform amplitude among the various wavelength-channels so that the amplitudes track for all steer angles. In the experimental results that follow

the dc biases of discrete wavelength lasers were adjusted to give equal optical amplitudes. In a practical antenna system driven by the tunable lasers in Figure 1, some amplitude errors will inevitably arise during the wavelength scanning, but those variations can be compensated for at the antenna plane by an equalization method in the electronic domain. The equalization technique is accomplished by adjusting the electrical bias of each preamplifier following each PD (and the bias of each LNA) so that the RF/microwave signal has the same amplitude at each antenna element. Post-detection electronics such as amplification, impedance matching, AGC circuitry, etc., is not shown, but is necessarily required with any phased array antenna.

4.2   Experimental Setup

Figure 2 shows our experimental system, constructed for the case of a linear array with N = 3 and M = 1. The FPG was designed to steer a three-element aperture to four positions: $0°$(broadside), $30°$, $59°$, and $60°$. Each of three single mode fibers contained a series of four Bragg gratings manufactured by 3M corporation. The peak grating reflection had spectral widths (FWHM) of 0.2 nm. The peak reflection wavelengths of the grating trios were 1552, 1553, 1557, and 1560 nm, respectively with the reflectivity of each greater than 70%. The individual gratings were 6.45 mm long (L_g in Figure 2). These fiber gratings were fed by an optical equal-arm "tree" splitter consisting of three 2 x 2 fused-fiber 3 dB couplers, c_1, c_2, and c_3 as shown. The spatial location d_{ij} of grating i along fiber j was as follows: $d_{11} = 0$, $d_{21} = 1.72$ cm, $d_{31} = 4.67$ cm, $d_{41} = 7.65$ cm, $d_{12} = 0$, $d_{22} = 3.44$ cm, $d_{32} = 7.62$ cm, $d_{42} = 10. 63$ cm, $d_{13} = 0$, $d_{23} = 5.16$ cm, $d_{33} = 10.57$ cm, and $d_{43} = 13.61$ cm. (This prism-shaped layout is shown in Figure 2). The optical return signals were routed by 3 dB fiber couplers c_4, c_5 and c_6 as shown, and directed to a spectrally broad Hewlett-Packard 11983 p-i-n lightwave converter (PD). Optical circulators were not used. Four thermally tunable diode lasers manufactured by Sea Star Inc., operating at 1552, 1553, 1557, and 1560 nm, were multiplexed on one optical feed to simulate one broadly tunable laser source (WML = Wavelength Multiplexed Laser). An AT&T model M2122AA Ti:LiNbO3 Mach-Zehnder amplitude modulator (EOM) was used to modulate the optical carrier with an RF signal whose frequency varied from 500 MHz to 4GHz. The EOM RF port was driven by a Hewlett-Packard 8753 6 GHz network analyzer. Our breadboard system included a polarization controller (PC) for the EOM, and an optical isolator (OI) at the WML output. The p-i-n detector output was fed into Port 2 of the Network Analyzer, which was used to gather time-delay data. Calibration of the measurement system, consisting of all of the above components except for the FGP was performed on the network analyzer and delay data was gathered using 1601 samples over the 3.5GHz bandwidth with no averaging.

Figure 3 shows the measured delay data (phase vs. frequency) for the FGP. Note from the figure that nine distinct non-zero delays are resolvable corresponding to the designed steer angles of $30°$, $59°$, and $60°$. A delay bias error exists caused by positioning accuracy of the BRG on the fiber that would cause the actual steer angle to differ slightly from design goal. Budgetary limitations dictated that the tolerance on the positioning of d_{ij} be held to ± 1mm or about 3%. In a final, fully engineered system, current BRG manufacturing technology can reduce this positioning error to as small a value as is necessary. The spurious-free dynamic range (SFDR) is used as a quality measure, though it should not be interpreted as best case, since a final, fully engineered system would likely perform better than the breadboard system measured here. For example, the AT&T modulator used has a nominal impedance of 43Ω, which resulted

in amplitude variations due to mismatch effects. The SFDR is determined in the conventional way via SFDR (dB) = (2/3)[IP_3 - N_o], where IP_3 is the third-order intercept point (in dBm), N_o is the total output noise and includes the effects of thermal noise, noise figure, and total system gain.
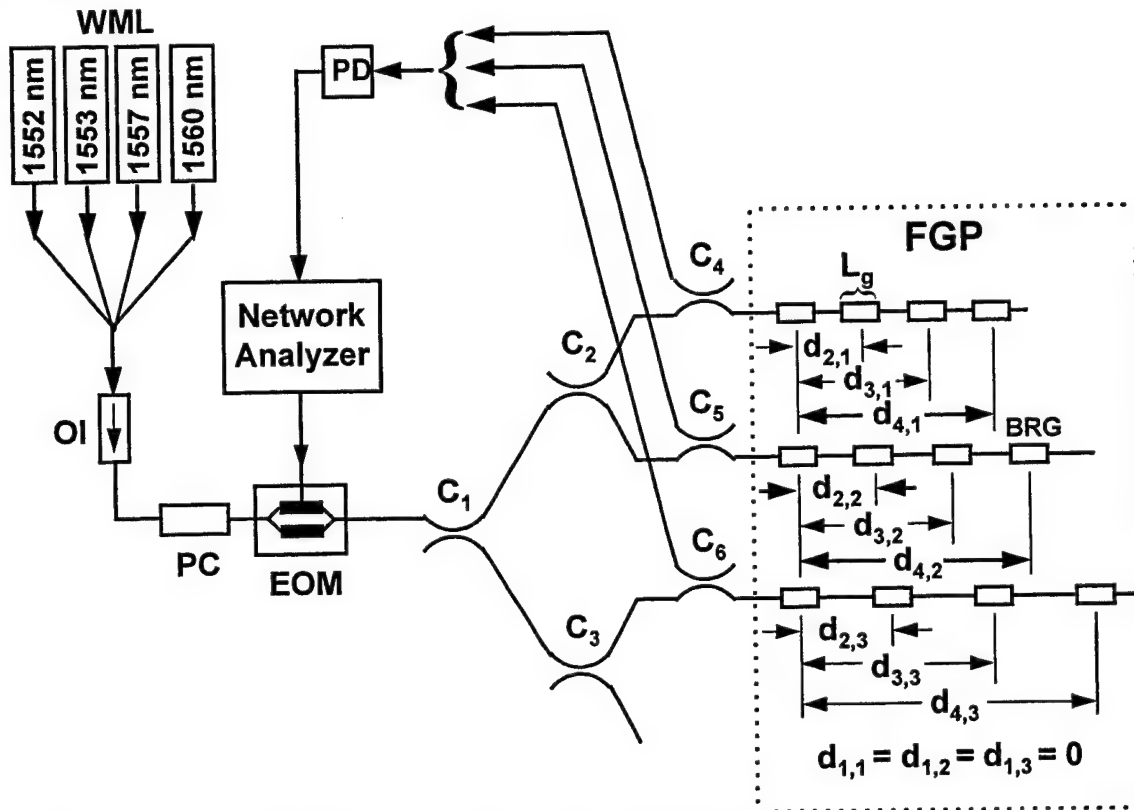

FIGURE 2: EXPERIMENTAL SETUP FOR THE DISCRETE BEAMFOMING SYSTEM.

The information for the noise figure was arrived at using a noise figure test set, and each leg of the FGP had a typical noise figure of 20 dB on average over the 3.5GHz band. Measured data for third order intermodulation products showed a SFDR of 42 dB/Hz. Measurements indicate that essentially all phase noise and nonlinear effects are due to the EOM as expected. The nominal phase noise (seen in the insert in Figure 3) shows a rms phase error of less than one degree over the 3.5GHz band, a result superior to any comparable electronic beamforming systems.

5 OTHER APPLICATIONS FOR FIBER GRATING SYSTEMS

5.1 Optical Packet Address Detection

The phased array receive application, when properly viewed as a matched filtering application, provides the motivation for using the fiber grating prism in a wide variety of related applications. For example, in packet based switching networks, which support different services with a potentially large range of attributes, a header attached to each packet contains a destination address in order to route the signal packet to the proper destination. Since the speed of address detection process at each switching node affects the network throughput significantly,

optical address detection systems have been sought to improve system performance [25]. The fiber optic prism allows for an efficient and novel implementation of this matched filtering function and is extremely well suited to function in the emerging WDM environment.
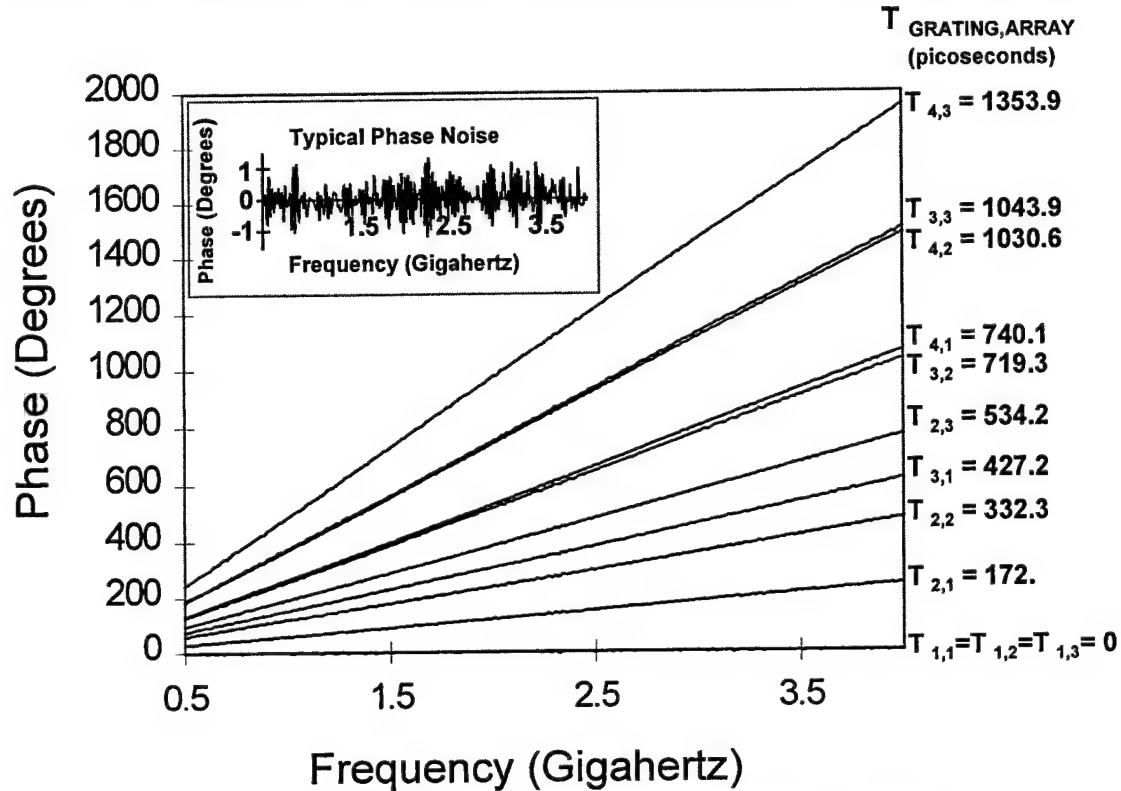

FIGURE 3: MEASURED DATA FOR THE DISCRETE BEAMFOMING SYSTEM.

Figure 4 shows the schematic diagram of an optical matched filter capable of encoding N distinct packet address codes, each at a different optical wavelength. An input optical pulse is split by couplers c_1, c_2, and c_3 into four identical pulses. The pulses are appropriately delayed (encoded) as determined by the physical placement of the BRG's on the optical fibers (which constitute the FGP) and then summed. This BRG placement determines the address code stored by the filter. Although the encoder portion shows a linear relationship among the location of BRG's of a given wavelength, any unique relationship can be used so long as the decoder is constructed accordingly.

The response y(t) of a matched filter with impulse response h(t) to input signal x(t) is given by the convolution of x(t) with h(t). If the incoming optical packet is identical to the address stored by the decoder except for a time-reversal, the filter output will the autocorrelation of x(t) resulting in a strong correlation. If the incoming packet and filter function are different, the filter output y(t) will be the cross-correlation between input signal x(t) and h(-t). Figure 4 shows the decoding process used for retrieving the information stored by wavelength λ_2. Similar decoders (not shown) would be used for other wavelengths. The determination of whether a particular bit stream is present is made using a threshold detection circuit as shown.

5.2 Transversal Notch Filtering

The advantages cited for using optical processing to control a phased array antenna also apply to the processing of wideband electronic signals for radar or other communications system applications where extremely wideband, low loss, lightweight analog filtering systems are required [23, 24]. Figure 5 shows the use of the FGP system as a non-recursive RF transversal notch filter. In figure 5, the RF modulated optical signal is split into two by couplers c_1, c_2 and c_3. Depending upon the optical wavelength λ_j, $j = 1,...,4$, the two legs experience four distinct differential time delays τ_j due to the spacing between BRG's. The back-reflected light is gathered by couplers c_2 and c_3, detected, and electrically summed to produce the desired RF output. A zero of transmission is obtained in the RF spectrum with its location selected by the laser wavelength. (The system shown in figure 5 has the ability to select four transmission zeros.) The
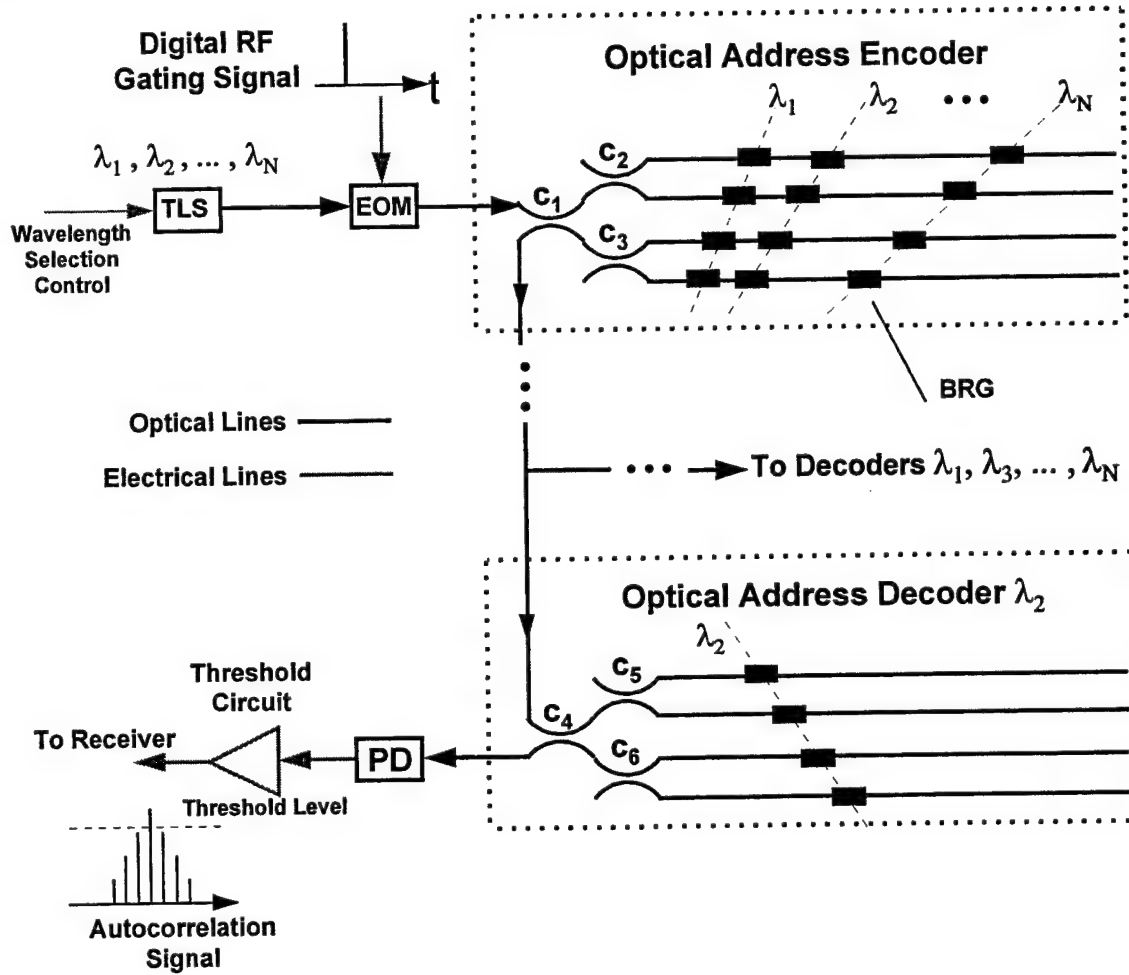

FIGURE 4: OPTICAL PACKET ADDRESS DETECTION SYSTEM

transfer function of this first-order transversal filter is given by

$$|H(f)| = 1 + \cos(2\pi f \, \tau_i(\lambda_i))$$

(9)

11

where f is the microwave frequency and τ_i is a differential time delay which depends on wavelength λ_i. Passband zeros will occur for frequencies which $2\pi f\tau = (2p+1)\pi$, p = 0,1,2,... . Reference points out that using separate detectors instead of combining optical signals into a single photodetector is necessary to avoid optical interference for lasers with a long coherence time. The first-order non-recursive filter discussed here is only one of many transversal-filtering architectures which exist in the signal processing literature. These other architectures may be implemented using ideas similar to those discussed above.
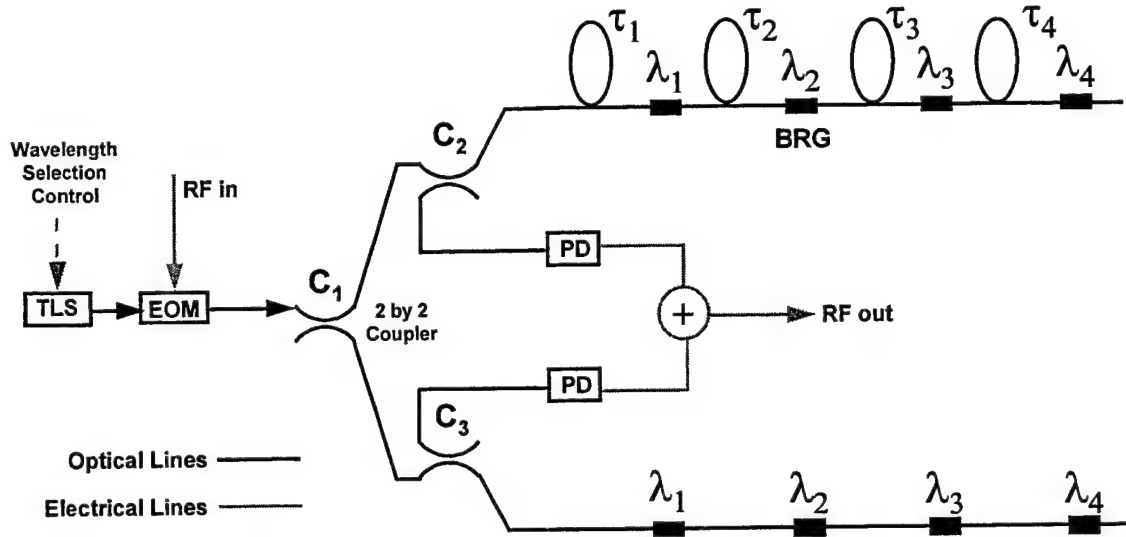

FIGURE 5: TRANSVERSAL NOTCH FILTER

6 OPTICAL CROSSBAR SWITCH ARCHITECTURE

6.1 Continuously Steered Arrays

A characteristic common to the above beamsteering or filtering systems is that the time delay varies in discrete increments with a fixed relationship between any two sets of BRG's arrays on the fiber. One notable application for which continuous beamsteering can dramatically improve system performance is that of null steering. This is where a zero of transmission of the array factor is aligned along a particular spatial coordinate. Such systems are used to minimize the signal degradation caused by multipath interference or to minimize the presence of an unwanted (and often dynamic) jamming signal(s). Such applications are currently receiving a good deal of attention for the case of GPS navigational systems. Other applications of continuously variable delay would include the ability to reconfigure the antenna radiation pattern (or filter transfer function) in an arbitrary manner, and this requires arbitrary independent delays. For tunable laser-based systems, continuously variable time delay is efficiently accomplished using High Dispersion Optical Fiber HDOF. As discussed in section 2.3, A microwave signal used to modulate an optical carrier with wavelength λ will undergo a time delay of

$$\tau(\lambda) = D \cdot \lambda \cdot L \qquad (10)$$

12

where D is the dispersion (in units of psec/nm-Km) and L is the length of the HDOF.
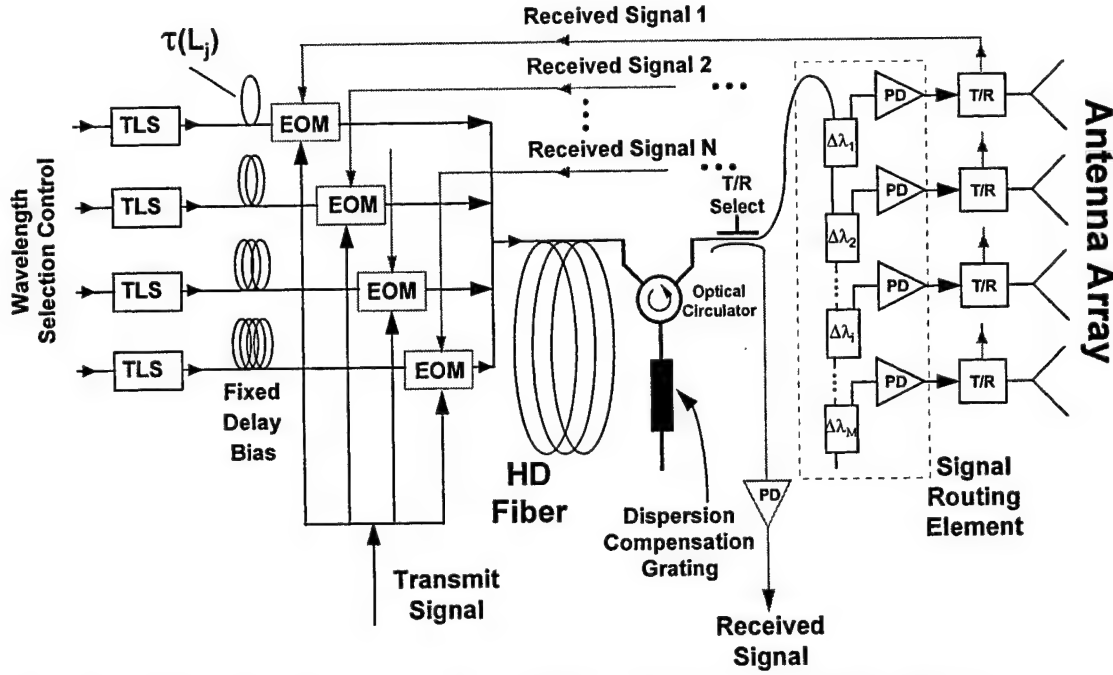

FIGURE 6: OPTICAL CROSSBAR SWITCH BEAMFORMING ARCHITECTURE.

An integrated transmit/receive continuously variable TTD beamformer which obtains the time delay from HDOF and uses BRG's as an wavelength demultiplexing arrangement is shown in figure 6. The transmit mode of operation is examined first. The figure shows a set of N modulated tunable wavelength lasers, each operating at a distinct wavelength λ_j, $j = 1, ..., N$. Each of these lasers is coupled to a fixed length of ordinary optical fiber of length L_j. The purpose of this fiber is to provide delay equalization and its value will be determined in the analysis which follows. The light leaving the delay equalization fibers are summed and coupled to a fixed length of HDOF of length L which provides a wavelength-dependent time delay $\tau(\lambda_j)$ obtained from equation (10).

This collection of optical signals, all of them now on a single optical fiber, are sent to the *signal routing element* (SRE), which acts as a wavelength demultiplexing system, and implemented as shown in figure (7) using broadband Bragg reflectors. It is seen in figure 7 that the signal, *f(t)* modulating wavelength λ_j with delay $\tau(\lambda_j)$ would pass through any gratings for which the wavelength λ_j fell outside the BRG's spectral passband $\Delta\lambda$ ($\lambda_j \notin \Delta\lambda$) and be reflected by the grating for which $\lambda_j \in \Delta\lambda$. The reflected signal is routed to the proper antenna element by an optical circulator or more efficiently with Mach-Zehnder based Bragg grating directional couplers which have an insertion loss of less than 0.5 dB with better than 99% coupling efficiency [26]. Even this loss limits the use of the present system for large arrays. For a large number of elements, an in-fiber Bragg grating tap can be used to replace the traditional broadband BRG's. These taps are fundamentally different from BRG's in that they couple light within a specific wavelength band into the fiber's cladding modes. This light can be extracted

13

from the cladding with roughly 10-20 % efficiency. More importantly, the off-wavelength transmission is still nearly 100% as with any fiber grating structure [27].
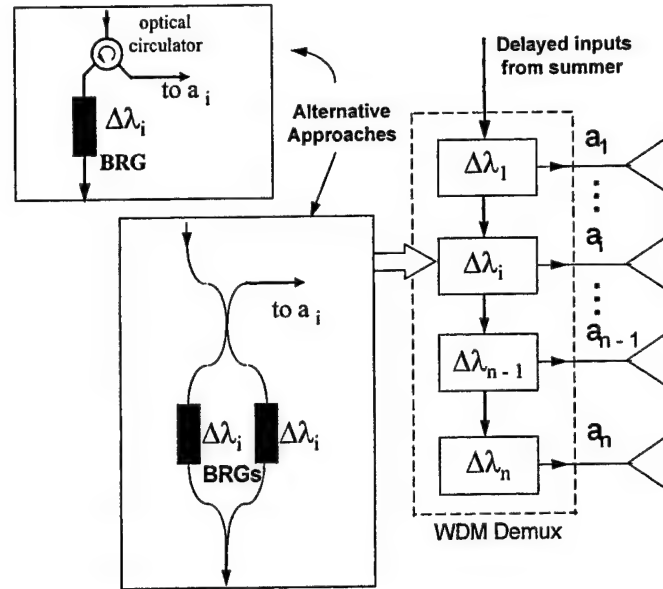

FIGURE 7: SIGNAL ROUTING ELEMENT.

As mentioned earlier, the purpose of the delay equalization fiber is to compensate for path length differences between all the lasers and the detectors. The total time delay T_j incurred by the microwave modulated optical signal emanating from laser j operating at wavelength λ_j and arriving at array location j computed from figure 6 as

$$T_j = \tau(L_j) + \tau(\lambda_j) + 2\tau_j + \tau_{j-1} + ... + \tau_1 \qquad (11)$$

where as before $\tau(L_j)$ is the fixed fiber delay at the laser j output, $\tau(\lambda_j)$ is the wavelength dependent delay obtained from the dispersion fiber, and τ_i is the delay through the i-th wavelength routing element. The required values of the fixed time delay equalization fiber lengths L_j is computed as follows. With all lasers operating at their respective center wavelengths, the time delay T_j (and hence L_j) is chosen so that a particular radiation pattern, generally a broadside pattern results.

One problem associated with optical fiber-based systems of this type, especially where long lengths of fiber are used, is the bandwidth limit imposed on the microwave signal by the fiber dispersion. Since ordinary fiber has dispersion D on the order of 20 picoseconds/nanometer-kilometer, this concern in compounded with the use of high dispersion fiber (D ≈ -100 ps/nm-km = -8 ps/GHz-km). This problem can be reduced and theoretically eliminated by including a linearly chirped Bragg grating at the output of the high dispersion fiber as shown in Figure 6. Such a device compresses the dispersion broadened pulses by providing an inverse to the chirp imposed by the high dispersion fiber [29]. Broad optical bandwidths may necessitate the use of several chirped gratings connected in series. Each device would possess the same chirp rate but centered at staggered wavelengths that cover the required optical band. If N EOM's are used for the transmit mode then an alternative approach may be taken. This would be to "pre-distort" the output of each EOM with a chirped grating covering only the portion of the

14

full spectral range tuned by one laser and compensate for the spreading that the signal will incur as it travels through the high dispersion fiber.

Array pattern synthesis techniques require that a continuous range of differential time delays $\Delta\tau_j$ be available to the array element. This range determines the spectral width $\Delta\lambda_j$ of the BRG passband, and is determined from Equation (10) as

$$\Delta\lambda_j = \frac{\Delta\tau_j}{D\,\ell} \tag{12}$$

The spectral passbands $\Delta\lambda_j$ for each array element are adjacent, with center wavelength λ_j. The tunable laser used to access array element j is operated at a center wavelength λ_j and has a tuning range of $\Delta\lambda_j$. This tuning range and center wavelength must be chosen so that the differential time delay $\Delta\tau_i$ necessary to drive array element i be obtainable from the HD fiber. For example, consider a linear 20 element antenna array with inter-element spacing of $\lambda_{RF}/2$. Assume a typical HDOF dispersion of D = -100psec/ nm·km. Additionally assume that the maximum steer angle desired is ± 60 degrees, which requires an inter-element delay of $(\lambda_{RF}/2c_o)sin(60^o)$. For a microwave signal wavelength λ_{RF} = 5 cm (f = 6 GHz) , the maximum inter-element delay (required by the last element) is about 832 psec. For a fiber grating passband $\Delta\lambda$ = 5 nm, equation (10) shows that the dispersive fiber length must be about 1.66 km.

Operation of the receive portion is simpler than that of the transmit portion of the system just described. Referring again to figure 6, the received microwave signals modulate the outputs of the TLS's which are summed and coupled into the HDOF where each received signal is appropriately time delayed. The optical T/R select switch directs the composite signal away from the SRE and into a spectrally broad photodetector. As seen in the figure the entire received signal delay is accomplished in a single element (the dispersive fiber) *after the signals are summed.* The ability to achieve efficient post summation signal delay is unique to the photonic processing approach shown here.

7   DYNAMIC NULL STEERING

7.1   Array Polynomial for a Null Steering Processor

It is well known that the directional characteristics of an N-element phased array may be expressed as a polynomial of degree (N - 1) (the array factor) and is given by:

$$AF_N(\theta) = \prod_{n=1}^{N-1}(z - z_n) = \sum_{n=0}^{N-1} a_n z^n \tag{13}$$

where $z = \exp\left[jkd\sin(\theta)\right]$ and where d is the antenna element spacing, $k = \omega/c$ is the free space wavenumber for radian frequency ω, c is the speed of light in free space, and $z_n = z(\theta_n)$ is a zero of the polynomial corresponding to a null at angular coordinate θ_n. Note that a change in location of even one zero affects *all* the polynomial coefficients a_n. This means that in order to independently place the *(N – 1)* array factor zeros requires *($2^{N-1} – 1$) independent* time delays.

15

Additionally, the precise element-to-element amplitude and phase tracking alluded to in the introduction must be maintained. These suggest that the ability to steer independent *broadband* nulls is much more complicated than that of a corresponding *narrowband* phased array. This is because as seen from Equation (13), a term of the form *exp[j k_od sin(θ_1) + j k_od sin(θ_2)]* requires a two delay line implementation to support broadband nulling. In the narrowband application however, a phase shifter can be used to obtain a typical coefficient a_n in the array factor polynomial, *but only at a single frequency*.

A multiple tunable laser-based broadband phased array receiver architecture that achieves the requirements imposed by Equation (14) is shown in Figure (9) for the case of a 4-element array. For tunable laser-based systems, continuously variable time delay is efficiently accomplished using a single High Dispersion Optical Fiber (HDOF). A microwave signal used to modulate an optical carrier with wavelength λ will undergo a time delay of $\tau(\lambda) = D \cdot \lambda \cdot L$ where D is the dispersion (in units of psec/nm-Km) and L is the length of the HDOF.

First note that for nulls located along angular coordinates θ_1, θ_2, and θ_3 the array factor takes the form

$$AF_4(\theta) = (e^{jkd \sin\theta} - e^{jkd \sin\theta_1})(e^{jkd \sin\theta} - e^{jkd \sin\theta_2})(e^{jkd \sin\theta} - e^{jkd \sin\theta_3})$$

$$= z^3 - z^2(e^{j\omega T_{21}} + e^{j\omega T_{22}} + e^{j\omega T_{23}}) + z(e^{j\omega T_{11}} + e^{j\omega T_{12}} + e^{j\omega T_{13}}) - e^{j\omega T_{01}}$$

$$= a_3 z^3 + a_2 z^2 + a_1 z + a_0$$

$$(14)$$
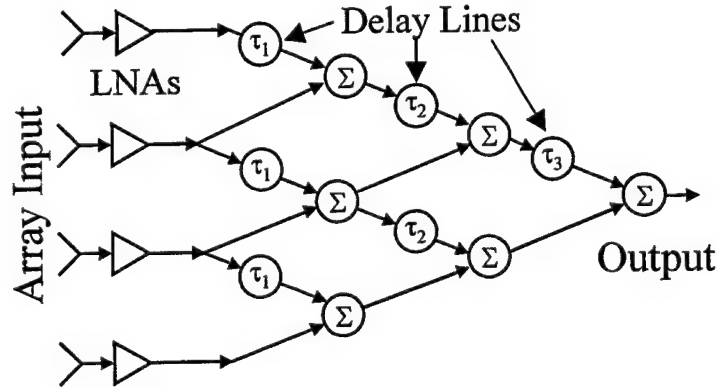
FIGURE 8: BROADBAND IMPLEMENTATION OF DAVIES NULLING.

where the required differential time delays with a_3 as the reference element are:

$$T_{21} = \frac{d}{c}\sin\theta_1, \ T_{22} = \frac{d}{c}\sin\theta_2, \ T_{23} = \frac{d}{c}\sin\theta_3, \ T_{11} = \frac{d}{c}(\sin\theta_1 + \sin\theta2),$$

$$T_{12} = \frac{d}{c}(\sin\theta_1 + \sin\theta_3), \ T_{13} = \frac{d}{c}(\sin\theta_2 + \sin\theta_3), \ T_{01} = \frac{d}{c}(\sin\theta_1 + \sin\theta_2 + \sin\theta_3). \quad (15)$$

Figure 8 shows a broadband realization of a nulling approach originally due to Davies [6]. The output of each element is split into two, and the outputs combined in adjacent pairs via identical time delays τ_1. The directional pattern of each element pair will be that of a two-element array and will produce one of the terms in the factored form of Equation (14). We now apply the same procedure to the outputs of the three new groupings, now with time delay τ_2, which produces the next factor in Equation (14). Continuing in this way the overall pattern $AF_N(\theta)$ is obtained.

The $N - 1$ delays required by Equation (13) are obtained using the bank of tunable lasers shown in Figure (9). Each laser operates at a wavelength $\lambda(T_{ij})$ and has a tuning range $\Delta\lambda$ wide enough so that the necessary differential time delays specified above can be accessed via the HDOF. The laser outputs are optically summed in the groups shown using optical couplers so that when delayed they form the appropriate polynomial coefficients a_0, a_1, a_2, and so on. Negative coefficients are obtained by using a broadband electrical pi-phase shifter at the appropriate modulator inputs, and amplifiers can be included to equalize the electrical signal level. The amplified signal from the antenna array element modulates the optical carrier using an Electrooptic Modulator (EOM). Direct modulation of the lasers are possible so long as this modulation does not introduce a wavelength shift or an RF phase shift. The EOM outputs are summed and coupled in a single length of HDOF which provides the desired wavelength dependent delay on each set of optical carriers. As previously noted this single length of HDOF makes the system insensitive to temperature variations and allows for close inter-element amplitude and phase tracking. The HDOF output is coupled to a spectrally broad photodetector (PD) which recovers the properly delayed and summed microwave antenna signals, which constitute the receiver output. For an adaptive system, a portion of this output as well as the outputs of each antenna elements would be digitized, and an appropriate algorithm would be used to adjust the laser operating wavelengths via the laser controller.

Regarding system loss, the optical power reaching the PD in Figure (9) is reduced by several factors. The major loss mechanisms are the couplers used to combine the laser outputs, with roughly 3-dB of loss for every two signals combined. The N : 1 summer used to combine the EOM outputs into the HDOF contributes a loss of *10 log N* dB plus excess loss, generally 1~2-dB. Generally, an EOM biased at quadrature contributes a total insertion loss of approximately 6 − 8 dB. The HDOF generally introduces a loss of 0.5 dB/km. Splices, connectors, isolators (if used) and the like will add another several dB of excess loss to the system. Since the system is fiber based, optical amplifiers can be incorporated into the design to compensate for the insertion losses of the system, however the effects of added noise would have to be examined. Post detection electronics such as impedance matching, AGC circuitry, and the like would also be present in any phased array system and is not shown in the figure.

7.2   Null Steering Breadboard System

Fig. 10 shows the experimental setup, constructed for the case of $N = 3$. Four thermally tunable diode lasers each with roughly a 2 nm tuning range were used as the optical sources. One laser always serves to provide a reference delay and need not be tunable. This reference laser and one other laser were coupled to individual EOM's while the outputs of the other two lasers were summed using optical coupler c_1 before being coupled into one EOM. Adjusting the laser drive

currents equalized the optical output power of the EOM's. The shared EOM was driven by an electrical signal with a broadband 180° hybrid junction to provide the negative polynomial coefficient in the array factor. The remaining two EOM's were also driven by the 0° output of
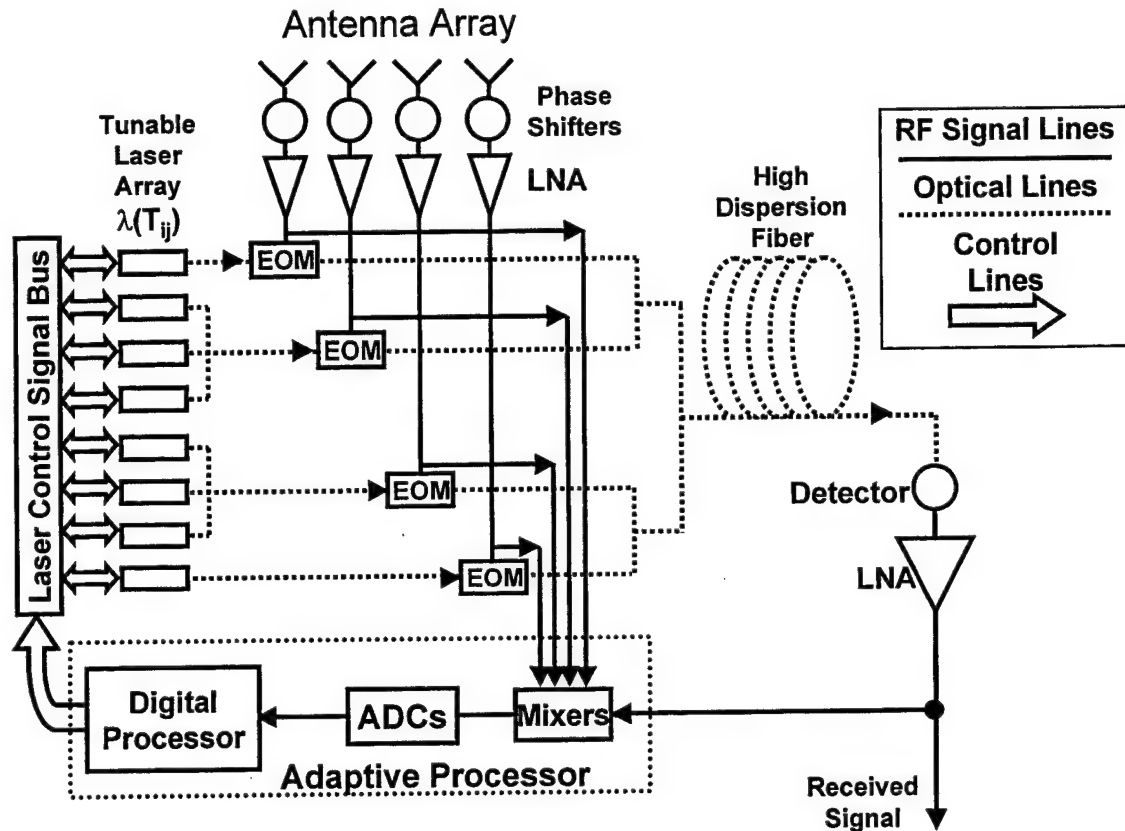

FIGURE 9: ADAPTIVE NULL STEERING PROCESSOR

identical hybrid junctions to maintain similar impedance characteristics. The effect of the spatially distributed array elements can be simulated by splitting the output signal of the RF network analyzer and introducing excess electrical path lengths between the EOM electrical inputs. For the measured data presented in the following section, an equal path length split was used to simulate a broadside signal incident on the array. The optical outputs of the three EOM's were summed using the couplers c_2, c_3, and c_4 shown with the output of coupler c_4 fused to a 5-km length of HDOF manufactured by Lucent Technologies with a dispersion of $D = -101.6$ psec/nm-km. A broadband photodetector followed by a 20dB RF amplifier drove port-2 of the network analyzer. The laser operating wavelengths were adjusted to provide nulls in the array factor at 0 and 60 degrees. Calibration of the measurement system described above was performed with respect to the reference laser and the necessary delay data was then measured using the network analyzer.

7.3 Experimental Results

Three nominally identical EOM modulators were used in the experimental setup shown in Figure 10, each capable of operating over a 7 GHz microwave bandwidth. Impedance measurements showed however that modulators had reasonably similar characteristics only over a 100 MHz bandwidth centered at 1.2 GHz (roughly the GPS center frequency), and this dictated the frequency range used in the measurements.

Figure 11 shows the performance of the three element nulling system versus frequency for the 3-element proof-of-concept breadboard described above. It is seen from the figure that a uniform null depth of roughly − 40dB is obtained across the full operating bandwidth. For comparison purposes only, Figure 11 also shows the null that results from and *ideal* phase shifter-based or narrowband system. From this comparison we see that an additional 20 dB of suppression is obtained at the band edges. Extending this null over a much larger bandwidth as well as increasing the null depth is possible with closely matched modulators and improved impedance matching at the antenna-modulator interface.
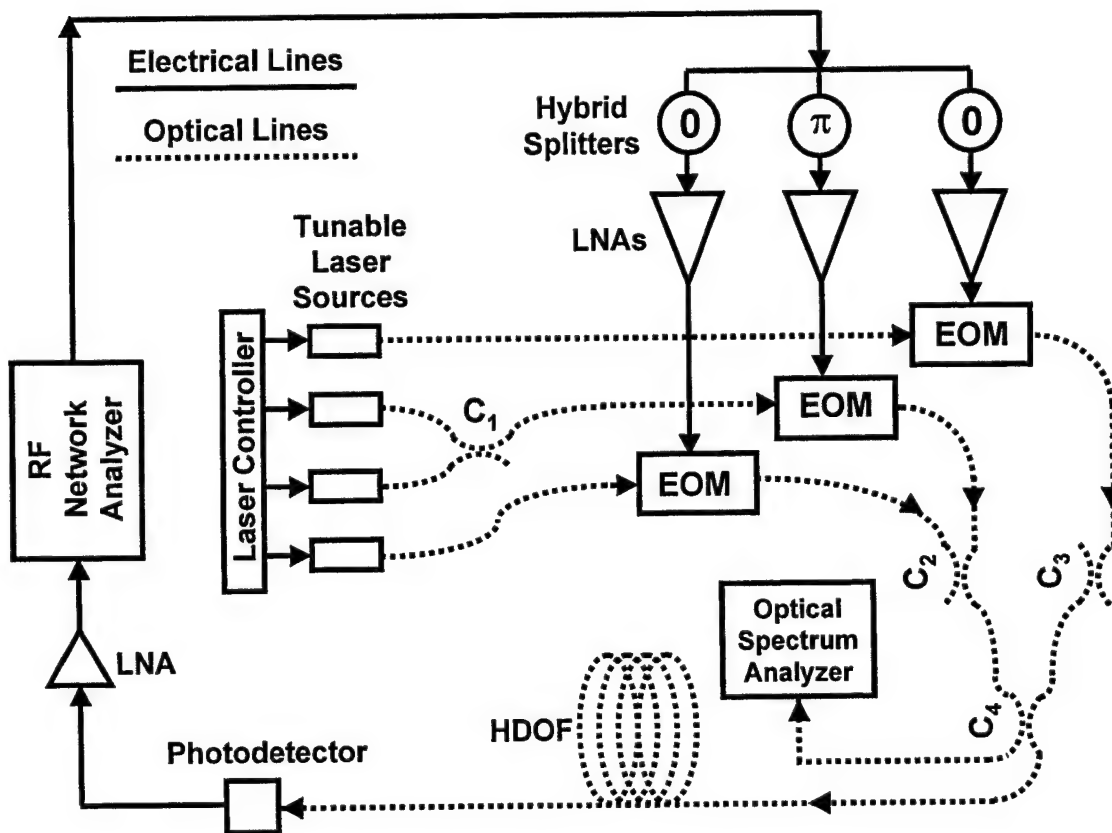

FIGURE 10: EXPERIMENTAL SETUP FOR NULL STEERING SYSTEM.
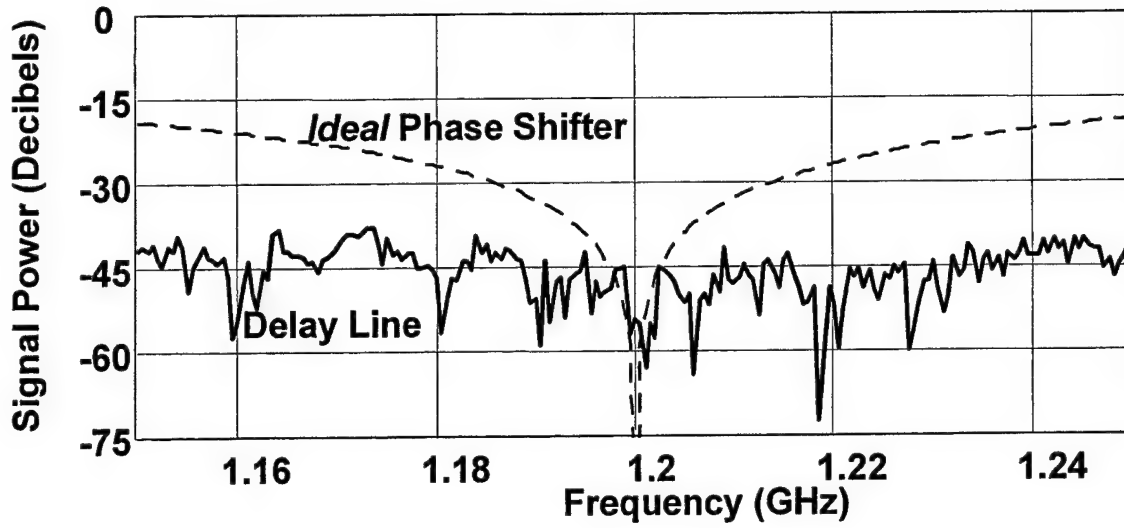
FIGURE 11: BROADBAND NULL STEERING EXPERIMENTAL RESULTS.

8   CLOSED-LOOP ADAPTIVE NULL STEERING WITH DELAY LINES[2]

We model three arbitrarily placed antenna elements receiving signals from three different directions as

$$X_1(t) = S_1(t - T_1) + S_2(t - T_2) + S_3(t - T_3)$$

$$X_2(t) = S_1(t - T_4) + S_2(t - T_5) + S_3(t - T_6)$$

$$X_3(t) = S_1(t - T_7) + S_2(t - T_8) + S_3(t - T_9) \qquad (16)$$

and we obtain the following three solutions for a single null placed in the direction of S_1.

$$Y_1(t) = X_1(t + T_1) - X_2(t + T_4) = S_2(t - T_2 + T_1) - S_2(t - T_5 + T_4) + S_3(t - T_3 + T_1) - S_3(t - T_6 + T_4)$$

$$Y_2(t) = X_1(t + T_1) - X_3(t + T_7) = S_2(t - T_2 + T_1) - S_2(t - T_6 + T_7) + S_3(t - T_3 + T_1) - S_3(t - T_9 + T_7)$$

$$Y_3(t) = X_2(t + T_4) - X_3(t + T_7) = S_2(t - T_5 + T_4) - S_2(t - T_6 + T_7) + S_3(t - T_6 + T_4) - S_3(t - T_9 + T_7)$$

$$(17)$$

Each solution yields two delayed copies of each of the remaining input signals S_2 and S_3. A second null is placed in the direction of signal S_2 as follows:

$$Z(t) = Y_1(t - T_8 + T_7) - Y_2(t - T_5 + T_4) + Y_3(t - T_2 + T_1)$$

$$= X_1(t + T_1 - T_8 + T_7) - X_2(t + T_4 - T_8 + T_7) - [X_1(t + T_1 - T_5 + T_4) - X_3(t + T_7 - T_5 + T_4)]$$
$$+ X_2(t + T_4 - T_2 + T_1) - X_3(t + T_7 - T_2 + T_1)$$

$$= X_1(t - u) - X_2(t - v) - X_1(t - w) + X_3(t - x) + X_2(t + y) - X_3(t - z)$$

$$= S_3(t - T_3) - S_3(t - T_1 + T_4 - T_6) - S_3(t - T_3 - T_5 + T_4 + T_8 - T_7)$$
$$+ S_3(t - T_1 - T_9 + T_8 - T_5 + T_4) + S_3(t - T_6 + T_4 - T_2 + T_8 - T_7) - S_3(t - T_9 - T_2 + T_8)$$

$$(18)$$

This is a unique solution, subject to a constant additive delay on each element As we increase the array size and the number of nulls, the process of canceling the residual components becomes exceedingly complex. Our results indicate that more than four antennas are required in order to place three independent nulls. Although $N-1$ independent narrowband nulls can be steered in an N-element array $N-1$ broadband nulls require more antenna elements and many more delay components.

For the linear array, with equally spaced elements, we let

$$T_1 = T_2 = T_3 = 0$$
$$T_7 = 2T_4$$
$$T_8 = 2T_5$$

and

$$T_9 = 2T_6$$

such that

$$Z_{linear}(t) = S_3(t) - S_3(t + T_4 - T_6) + S_3(t + T_4 + T_5 - 2T_6) - S_3(t - T_4 + T_5) + S_3(t - T_4 + 2T_5 - T_6) - S_3(t + 2T_5 - 2T_6)$$

$$(19)$$

Again we have six residual signal components of S_3. By using Davies' technique of successive cancellation we obtain

$$Z_{Davies}(t) = X_1(t) - X_2(t + T_4) - X_2(t + T_5) + X_3(t + T_4 + T_5)$$

$$= S_3(t) - S_3(t + T_4 - T_6) + S_3(t + T_4 + T_5 - 2T_6) - S_3(t + T_5 - T_6)$$

$$(20)$$

We see that this is a different solution with four residual components rather than the six we had before. We also see that the first three residual components are present in both solutions. Thus, two entirely different solutions are possible using the linear array.

In a narrowband antenna array there is a unique solution, the Wiener solution, which minimizes the array output power subject to a gain constraint. Several algorithms are available to implement this solution in adaptive null steering systems. We now consider whether it is possible to map the Wiener solution to the time delay solution. Let us assume a three-element arbitrary array with unit weight on $X_1(t)$. The Wiener solution applies complex weights to $X_2(t)$ and $X_3(t)$. If we consider high signal to noise ratios, i.e., approximately zero additive noise, then the Wiener solution will place zeros in the directions of the two signal sources if only two are present. If more sources are present, then nulls will not generally lie in the directions of the signal sources. Successive cancellation also produces the Wiener solution only when two sources are present. Otherwise, the output power is not minimized and we will say that the array is overdriven by the number of signal sources. Assuming the array is not overdriven, we construct a polynomial representation of the antenna patterns as follows:

First we map the delay to a phase shift at an assumed frequency. For the successive cancellation method we obtain

$$Z_{Davies}(t) = X_1(t) - X_2(t+T_4) - X_2(t+T_5) + X_3(t+T_4+T_5)$$

$$= X_1(t) - (exp(j2\pi T_4/\lambda) + exp(j2\pi T_5/\lambda))X_2(t) + exp(j2\pi T_5/\lambda)\ exp(j2\pi T_4/\lambda)X_3(t)$$

$$= X_1(t) - exp(j2\pi T_4/\lambda)X_2(t) - exp(j2\pi T_5/\lambda)\{X_2(t) - exp(j2\pi T_4/\lambda)X_3(t)\} \tag{21}$$

If noise is negligible, the time delay and Wiener Solutions are identical since they both minimize power.

The gain is expressed as

$$AF_3(\theta) = [exp(jkd\ sin\ \theta) - exp(jkd\ sin\ \theta_1)]\ [exp(jkd\ sin\ \theta) - exp(jkd\ sin\ \theta_2)] \tag{22}$$

Where $kd\ sin\ \theta_1 = j2\pi T_4/\lambda$ and $kd\ sin\ \theta_1 = j2\pi T_4/\lambda$. We simplify this expression as follows:

$$AF_3(\theta) = a_2z^2 + a_1z^1 + a_0 \tag{10}$$

Given a Wiener solution in this form, we can obtain the roots of the polynomial and map them easily to the delay parameters. It is rather cumbersome to implement an adaptive algorithm to find the Wiener solution and to follow it with a root-solving algorithm. A direct search for the delays is much more efficient.

Level curves of the array output power given two variable delays and two signal sources are shown in Figure 12. These level curves assume independent signal sources with autocorrelation functions of the following form:

$$R(t) = P_{avg}exp[-|t|(j/\tau_1 + 1/\tau_2)] \tag{23}$$

We set the fractional bandwidth, $2\tau_2/\tau_1$ to a value of 1/30 to model a 50 MHz broadband noise source at the GPS L1 center frequency of 1575 MHz. The signals arrive with delay offsets of 0.1 and 0.3 times the carrier period.

We note that the power surface indicates two zeros as global minimums and repeated nonzero local minimums at wavelength offsets. The local minimums occur as a result of the periodicity of the signal autocorrelation functions. Clearly, we can use a gradient search technique to find one of the minimums if we properly constrain the region of observation to within a wavelength centered about the origin.

The LMS algorithm is commonly used to iteratively find the Wiener solution. With each iteration of the algorithm, a single sample of the input data and a single sample of the array output are used to estimate the gradient. The system weights are then adjusted in the opposite direction of the gradient. When implementing time delays, we cannot estimate the gradient direction using a single measurement of the data and the array output. Rather we must test several trial solutions. Thus, we expect any time delay algorithm to require more samples of data to be evaluated in order to converge to a solution.

We also note that the error surface shown in Figure 12 contains plateaus where the magnitude of the gradient approaches zero. This tends to cause the search algorithm to proceed more slowly when searching these regions since the signal to noise ratio of the gradient estimate is low.

Assuming a laser with a 50-nanometer tuning range, the required length of HDOF introduces a delay of approximately 1 μsec. This is the minimum possible iteration period. If we sample the signals at twice the GPS data rate we will obtain new data every 50 nanoseconds. Thus, we can implement 1000/50 = 20 trial solutions with each iteration using a single dispersive fiber. We are currently evaluating direct search algorithms that will make efficient use of these trial solutions and rapidly locate one of the global minimums.
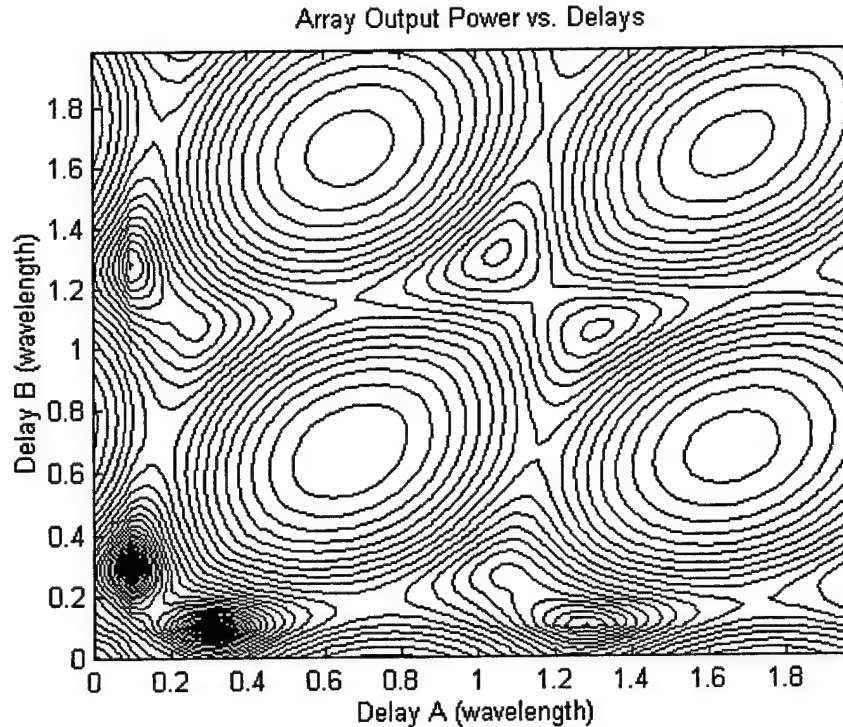
Array Output Power vs. Delays

FIGURE 12: OUTPUT POWER AS A FUNCTION OF DELAYS. NULLS ARE LOCATED AT 0.1 & 0.3.

9   CONCLUSIONS AND FUTURE DIRECTIONS

Presented here are several new and simple systems for wideband dynamic processing of high-speed signals, with special attention given to the application of true-time-delay beamsteering of phased array antennas including null steering. These photonic processors rely heavily on relatively new and very efficient photonic components, specifically in-fiber Bragg reflection gratings. Because of the versatility of these BRG's with regard to reflection bandwidth and reflectivity, they are rapidly becoming a fundamental optical signal processing element. When used in conjunction with wavelength-tunable laser sources, arrays of BRG's can be designed to form a fiber grating prism. A discrete true-time-delay beamforming system for phased array antenna employing such a prism was breadboarded and experimental data was presented which demonstrated 3.5GHz bandwidth high resolution beamsteering with highly linear low-noise phase data.   It was further shown how, when properly interpreted from a matched filtering standpoint, this same data infers that the fundamental topology of a fiber grating prism can be used to address other aspects for optical processing of high-speed signals such as optical packet header encoding/decoding for WDM telecommunications and transversal microwave filtering. Although illustrated as fiber-based, many of the systems presented can be integrated on a single substrate in the form of a photonic integrated circuit. Finally it was shown how a BRG array can serve as a key element in a *continuously variable* true-time-delay system for phased arrays, where the time delay information is obtained using the well-understood component of high-dispersion optical fiber. A breadboard system of this type, specifically directed toward antenna array null steering for GPS anti-jam applications is planned for implementation at the Air Force Research Laboratory (formerly Rome Laboratory) Photonics

Center in the near future. The systems presented are expected meet all the rigorous requirements necessary for defense applications yet have the potential to be inexpensive enough to make them attractive to the commercial sector.

The requirement of having $(2^{N-1} - 1)$ tunable lasers clearly limits the present system to that of small order arrays $(N \sim 6)$. Such low-order systems have wide applicability in many telecommunications and navigation applications where small platforms constrain the array size. The ability to obtain a given null depth over a specified bandwidth is primarily governed by how well the impedance characteristics of the EOM's are matched to each other over the desired bandwidth. The depth of the null itself is also influenced by noise. The length of HDOF introduces a lever arm effect, which enhances laser wavelength jitter effects. Hence for a given laser characteristic, a wide tuning range is preferred to long lengths of HDOF. Commercially available tunable lasers have tuning ranges in excess of 80nm and would have reduced the required HDOF length in the experimental setup by a factor of forty.

The thrusts for future effort in this are threefold. First will be to construct and test a system beyond the breadboard (proof-of-concept) level to assess the systems suitability in real Air Force applications. Another obvious area for improvement is to reduce the need for $2^{N-1} - 1$ tunable lasers down to a number reasonable for even modest sized arrays. This investigation is currently underway and will most likely involve a tradeoff between system complexity and number of lasers. It may, for example, require the use of more than one high-dispersion optical fiber. How this impacts upon issues such as temperature stability is be a factor in the investigation.

Finally an area of great interest is the applicability of the systems proposed for conformal array architectures. Presently, it has been seen that the system complexity increases dramatically when the planar (linear) array assumption is relaxed. The ability to achieve an efficient broadband conformal array processor has eluded researchers for years and continues to be an open research topic.

10 Publications and Patents Resulting from the Effort

Richard A. Soref and Henry Zmuda, "Apparatus for Photonic Time-Delay Beamsteering System Using Fiber Bragg Prism", Patent Pending, Air Force Invention Number AFB00304, 1998.

N.A. Riza, Editor, *Selected Papers on Photonic Control Systems for Phased Array Antennas*, SPIE Milestone Series Volume MS 136, Bellingham, Washington: SPIE Optical Engineering Press, 1997, pp.32-34.

H. Zmuda, E.N. Toughlian, P. Payson, and H. Klumpe, III, "A Photonic Implementation of a Wideband Nulling System for Phased Arrays", IEEE Photonics Technology Letters, Vol. 10, No. 5, pp. 725-727, May 1998.

H. Zmuda, E.N. Toughlian, P. Payson, and H. Klumpe, III, "A Photonic True Time Delay Processor for GPS Null Steering", *Invited Paper*, IEEE Aerospace Conference, Aspen CO, March 21-28, 1998, 7 pages.

H. Zmuda, E.N. Toughlian, P. Payson, S. Johns, and R.A. Soref, "Photonic Beamformer for Phased Array Antennas Using a Fiber Grating Prism", IEEE Photonics Technology Letters, vol. 9, no. 2, pp. 241-243, February 1997.

H. Zmuda, E.N. Toughlian, P. Payson, and H. Klumpe, III "Dynamic Null Steering for Broadband Phased Array Antennas via Photonic Processing", *Invited Paper*, SPIE Proceedings, Vol. 3463, (Photonics and Radio Frequency), July 1998, 9 pages.

H. Zmuda, E.N. Toughlian, P. Payson, and H. Klumpe, III, "Dynamic Null Steering for Broadband Phased Array Antennas via Photonic Processing", *Invited Paper*, SPIE Proceedings, Vol. 3384, (Photonic Processing Technology and Applications), April 1998, pp. 80-88.

H. Zmuda, E.N. Toughlian, P. Payson, S. Johns, and R.A. Soref, "Photonic Crossbar Switch Architecture for Phased Array Beamforming Applications", *Invited Paper*, SPIE Proceedings, Vol. 3075 (Photonic Processing Technology and Applications), April 1997, pp. 89-100.

H. Zmuda, E.N. Toughlian, P. Payson, and H. Klumpe, III, "A Photonic Broadband Adaptive Nulling Processor for Phased Array Antennas", The Eighth Annual DARPA Symposium on Photonic Systems for Antenna Applications, Monterey CA, January 1998, 4 pages.

H. Zmuda, E.N. Toughlian, P. Payson, S. Johns, and R.A. Soref , "Photonic Beamformer for Phased Array Antennas Using a Wavelength Dependent Crossbar Switch Architecture", The Seventh Annual DARPA Symposium on Photonic Systems for Antenna Applications, Monterey, CA, January 1997, pp. 179-184.

11 REFERENCES

1. N.A. Riza, editor, *Selected Papers on Photonic Control Systems for Phased Array Antennas*, Bellingham, Washington: SPIE Optical Engineering Press, 1997.

2. H. Zmuda, and E.N. Toughlian, editors, *Photonic Aspects of Modern Radar*, Dedham, Massachusetts: Artech House Publishers, 1994.

3. M.Y. Frankel and R.D. Esman, *True Time-Delay Fiber-Optic Control of an Ultrawideband Array Transmitter/Receiver with Multibeam Capability*, IEEE Transactions on Microwave Theory and Techniques, Vol. 43, No. 9, September 1995, pp.2387-2394.

4. R.A. Soref, *Optical Dispersion Technique for Time-Delay Beam Steering*, Applied Optics, Vol. 31, No. 35, 10 December 1992, pp. 7395-7397.

5. B.D. Carlson, L.M. Goodman, J. Austin, M.W. Ganz, and L.O. Upton, *An Ultralow-Sidelobe Adaptive Array Antenna*, Lincoln Laboratory Journal, Vol. 3, No. 2, 1990, 17 pp.

6. D.E.N. Davies, *Independent Angular Steering of Each Zero of the Directional Pattern for a Linear Array*, IEEE Transactions on Antennas and Propagation, March 1967, pp. 296-298.

7. Haykin, S. Adaptive Filter Theory (Second Edition), Prentice Hall, Englewood Cliffs, NJ. 1991.

8. S.T. Johns, D.A. Norton, C.W. Keefer, R. Erdmann, and R.A. Soref, *Variable Time Delay of Microwave Signals Using High Dispersion Fiber*, Electronics Letters, Vol. 29, No. 6, 18th March 1993, pp. 555-556.

9. R.J. Campbell and R. Kashyap, *The Properties and Applications of Photosensitive Germanosilicate Fibre,* International Journal of Optoelectronics, Vol. 9, No. 1, 1994, pp. 33-57.

10. M.C. Farries, K. Sugden, D.C.J. Reid, I. Bennion, A. Molony, and M.J. Goodwin, Very Broad Reflection Bandwidth (44nm) Chirped Fibre Gratings and Narrow Bandpass Filters Produced by the use of an Amplitude Mask, Electronic Letters, Vol. 30, No. 11, 1994, pp. 891-892.

11. G.A. Ball, W.H. Glenn and W.W. Morey, *Programmable Fiber-Optic Delay Line,* IEEE Photonics Technology Letters, Vol. 6, No. 6, June 1994, pp.741-743.

12. Moloney, C. Edge, and I. Bennion, *Fibre Grating Time Delay Elements for Phased Array Antennas*, Electronics Letters, Vol. 31, No. 17, 17th August 1995, pp.1485-1486.

13. R.A. Soref, *Fiber Grating Prism for True Time Delay Beamsteering*, Fiber and Integrated Optics, Vol. 15, No. 4, October 1996, pp. 325-333.

14. Mailloux, R.J., Phased Array Antenna Handbook, Boston: Artech House, 1994.

15. P. Zoribedian, *External Cavity Tunable Lasers*, in: A.J. Duarte, Editor, Tunable Laser Technology, New York: Academic Press, 1995.

16. M.Y. Frankel, R.D. Esman, and J.F. Weller, *Rapid Continuous Tuning of a Single-Polarization Fiber Ring Laser*, IEEE Photonics Technology Letters, Vol. 6, No. 5, May 1994, pp. 591-593.

17. Kuznetsov, M., *Design of widely tunable semiconductor three-branch lasers*, IEEE Journal of Lightwave Technology, Vol. 12, No. 12, Dec. 1994, pp. 2100-2106.

18. B. Glance, U. Koren, C.A. Burrus, J.D. Evankov, *Discretely-Tuned N-Frequency Laser for Packet Switching Applications Based on WDM*, Electronics Letters, Vol. 27, No. 15, 18th July 1991, pp. 1381-1383.

19. M. Morinaga, M. Ishikawa, and N. Suzuki, *Analysis on Wide Continuous Wavelength Tuning of Rapid-Tunable Quantum-Well DFB Lasers with Carrier-Transport Effects*, IEEE Journal of Selected Topics in Quantum Electronics, Vol. 1, No. 2, June 1995, pp. 427-432.

20. Y. Tohmori, F. Kano, H. Ishii, Y. Yoshikuni, and Y Kondo, *Wide Tuning with Narrow Linewidth in DFB Lasers with Superstructure Grating (SSG)*, Electronic Letters, Vol. 29, No. 15 July 22nd, 1993, pp. 1350-1351.

21. Kim, R.C. Alferness, U. Koren, L.L. Buhl, B.I. Miller, M.G. Young, M.D. Cohen, T.L. Kock, H.M. Presby, G. Raybon, and C.A. Burrus, *Broadly Tunable Verical-Coupler Filtered Tensile-Strained InGaAs/InGaAsP Multiple Quantum Well Laser*, Applied Physics Letters, Vol. 64, No. 21, 23 May 1994, pp. 2764-2766.

22. H. Okamoto, H. Yasaka, K. Sato, Y. Yoshikuni, K. Oe, K. Kishi,. Y. Kondo, and M. Yamamoto, *A Wavelength-Tunable Duplex Integrated Light Source for Fast Wavelength Switching*, IEEE Journal of Lightwave Technology, Vol. 14, No. 6, June 1996, pp. 1033-1041.

23. M.Y. Frankel and R.D. Esman, *Fiber-Optic Tunable Microwave Transversal Filter*, IEEE Photonics Technology Letters, Vol. 7, No. 2, Feb. 1995, pp. 191-193.

24. F. Coppinger, S. Yegnanarayanan, P.D. Trinh, B. Jalali, and I.L. Newberg, *Nonrecursive Tunable Photonic Filter Using Wavelength-Selective True Time Delay*, IEEE Photonics Technology Letters, Vol. 8, No. 9, Sept. 1996, pp.1214-1216.

25. J.D. Shin, M.Y. Jeon, and C.S. Kang, Fiber-Optic Matched Filters with Metal Films Deposited on Fiber Delay-Line Ends for Optical Packet Address Detection, IEEE Photonic Technology Letters, Vol. 8, No. 7, July 1996 pp. 941-942.

26. F. Bilodeau, D.C. Johnson, S. Thériault, B. Malo, J. Albert and K.O. Hill, *An all-fiber, dense wavelength division multiplexer / demultiplexer using photoimprinted Bragg gratings*, IEEE Photonics Technology Letters, 1995, Vol 7, No 4, p. 388.

27. G. Meltz, W.W. Morey, and W.H. Glenn, *In-Fiber Bragg Grating Tap*, in Technical Digest on Optical Fiber Communication, Optical Society of America, Washington, D.C., 1990, p.24.

28. H. Zmuda, R.A. Soref, P. Payson, S. Johns, and E.N. Toughlian, *Photonic Beamformer for Phased Array Antennas Using a Fiber Grating Prism,* IEEE Photonics Technology Letters, Vol. 9, No. 2, 99241-243, Feb. 1997.

29. F. Ouellette, Dispersion Cancellation Using Linearly Chirped Bragg Grating Filters in Optical Waveguides, Optics Letters, Vol. 12, No. 10, pp. 847-849, Oct. 1987.